

**Further new borosulfates: synthesis, crystal structure, and vibrational spectra of  $A[B(SO_4)_2]$  ( $A = Na, K, NH_4$ ) and the crystal structures of  $Li_5[B(SO_4)_4]$  and  $NH_4[B(S_2O_7)_2]$**

**Michael Daub, Henning A. Höppe, Harald Hillebrecht**

**Angaben zur Veröffentlichung / Publication details:**

Daub, Michael, Henning A. Höppe, and Harald Hillebrecht. 2014. "Further new borosulfates: synthesis, crystal structure, and vibrational spectra of  $A[B(SO_4)_2]$  ( $A = Na, K, NH_4$ ) and the crystal structures of  $Li_5[B(SO_4)_4]$  and  $NH_4[B(S_2O_7)_2]$ ." *Zeitschrift für anorganische und allgemeine Chemie* 640 (14): 2914–21.  
<https://doi.org/10.1002/zaac.201400315>.



# Further New Borosulfates: Synthesis, Crystal Structure, and Vibrational Spectra of $A[B(SO_4)_2]$ ( $A = Na, K, NH_4$ ) and the Crystal Structures of $Li_5[B(SO_4)_4]$ and $NH_4[B(S_2O_7)_2]$

Michael Daub,<sup>[a]</sup> Henning A. Höppe,<sup>\*[c]</sup> and Harald Hillebrecht<sup>\*[a,b]</sup>

*Dedicated to Professor Martin Jansen on the Occasion of His 70th Birthday*

**Keywords:** Crystal structure; Vibrational spectroscopy; Borosulfate; Borates; Sulfate

**Abstract.** The reaction of alkali sulfates and boron oxide in oleum yielded the complexes  $A[B(S_2O_7)_2]$  ( $A = Li, Na, K, NH_4$ ). This way we obtained the first ammonium-containing borosulfate and we determined the crystal structure.  $NH_4[B(S_2O_7)_2]$  [ $Cc, Z = 8, a = 11.4403(2), b = 14.9439(2) c = 13.8693(2) \text{ \AA}$ ] crystallizes isotyp to  $K[B(S_2O_7)_2]$ . Thermal decomposition or treatment in vacuo resulted in compounds with composition  $A[B(SO_4)_2]$ . One-dimensional chain structures are obtained for  $A = Na, K, NH_4$ .  $NH_4[B(SO_4)_2]$  [ $P4/ncc, Z = 4, a = 9.1980(1), c = 7.4258(1) \text{ \AA}$ ] and  $K[B(SO_4)_2]$  [ $P4/ncc, Z = 4, a = 8.9739(3), c = 7.4114(3) \text{ \AA}$ ] are isotyp with  $H_3O[B(SO_4)_2]$ . The chains

of edge-sharing “ $BS_4$  super tetrahedra” have  $\bar{4}$  symmetry. In  $Na[B(SO_4)_2]$  [ $P2/c, Z = 2, a = 5.434(5), b = 7.570(7) c = 7.766(8) \text{ \AA}, \beta = 108.56(3)^\circ$ ] the chain is twisted.  $Li_5[B(SO_4)_4]$  [ $P2_1/c, Z = 4, a = 8.0191(1), b = 10.1211(1) c = 15.0401(2) \text{ \AA}, \beta = 104.033(1)^\circ$ ] contains isolated pentameric unit and represents a new structure type.  $Li_5[B(SO_4)_4]$  was obtained from  $Li[B(S_2O_7)_2]$  with additional  $Li_2SO_4/SO_3$ . Vibrational spectra of  $A[B(S_2O_7)_2]$  ( $A = Na, K, NH_4$ ) are presented and force constants calculated. In all structures  $BO_4$  and  $SO_4$  tetrahedra are connected by common apices forming  $BS_4$  super tetrahedra.

## Introduction

Borosulfates are a very young and rapidly growing class of compounds. In 2012  $K_5[B(SO_4)_4]$  was characterized as the first example. Up to now 12 compounds are known with seven different topologies for the anions.<sup>[1–3]</sup> In analogy to borophosphates<sup>[4]</sup> a classification based on the B:S ratio is useful.<sup>[3,4]</sup> With a B:S ratio of 1:4 non-condensed borosulfates are found like the open branched pentameres in  $A[B(SO_4)_4]$  ( $A = Na, K$ )<sup>[2,3]</sup> and the loop- or cyclo-branched pentameric anions in  $A[B(S_2O_7)_2]$  ( $A = Li - K$ ).<sup>[3]</sup> With a ratio 1:3 chain structures are formed like the open branched “vierer” single chains in  $A_3[B(SO_4)_3]$  ( $A = K, Rb$ )<sup>[2]</sup> or the cyclo branched “vierer” single chains in  $A[B(SO_4)(S_2O_7)]$  ( $A = H, Cs$ ).<sup>[3]</sup> With a ratio of 1:2 also chain structures as the loop branched “vierer” single

chain in  $H_3O[B(SO_4)_2]$ <sup>[3]</sup> are found but also framework structures were observed in  $Li[B(SO_4)_2]$ <sup>[2]</sup> homeotypic with  $SiO_2$  (tridymite). All these compounds only contain B–O–S bridges and in the case of disulfate complexes also S–O–S bridges. To obtain B–O–B bridges, i.e. the connection of  $BO_4$  tetrahedra, it seems to be necessary to reduce the B:S ratio below 1:2 as done for  $B_2S_2O_9$ <sup>[5]</sup> that adopts a layer structure with phyllosilicate topology. Independent from the B:S ratio there are two aspects which enable different topologies. Firstly there is interplay between sulfate and disulfate groups, which changes the charge of the borosulfate building units. Secondly, the dimensionality can be different according to the mode of connection. So with a B:S ratio of 1:2 a 3D structure ( $Li[B(SO_4)_2]$ ) or a 1D chain structure ( $H_3O[B(SO_4)_2]$ ) can be realized. Because up to now all borosulfates base on tetrahedral units sharing common corners there is a close similarity to the structures of silicates.<sup>[6]</sup> Furthermore, the method of *Balić Žunić* and *E. Makovicky*<sup>[7]</sup> allows to quantify deviations from an idealized tetrahedral arrangement. This method can also be used to characterize distortions of the tetrahedral framework. As all borosulfates have  $BO_4$  tetrahedra which are connected to four  $SO_4$  tetrahedra by common apices one can define “ $BS_4$  super tetrahedra”.

According to the reaction conditions the ratio B:S can be biased. In general higher temperatures favor a lower B:S ratio according to the evaporation of  $SO_3$ . Furthermore, the use of oleum as a medium for the reaction promotes the formation of disulfates and compounds with a high B:S ratio.<sup>[2,3]</sup> On the

\* Prof. Dr. H. A. Höppe

E-Mail: henning.hoepp@physik.uni-augsburg.de

\* Prof. Dr. H. Hillebrecht

E-Mail: harald.hillebrecht@ac.uni-freiburg.de

[a] Institut für Anorganische und Analytische Chemie  
Albert-Ludwigs-Universität  
Albertstraße 21  
79104 Freiburg, Germany

[b] Freiburger Materialforschungszentrum FMF  
Albert-Ludwigs-Universität  
Stefan-Meier-Straße 25  
79104 Freiburg, Germany

[c] Institut für Physik Universität Augsburg  
Universitätsstr. 1  
86159 Augsburg, Germany

Supporting information for this article is available on the WWW under <http://dx.doi.org/10.1002/zaac.201400315> or from the author.

other hand, it is possible to obtain borosulfates with a high B:S ratio by reacting suitable starting materials with oleum.

The influence of the cations, which are monovalent in our compounds, plays a secondary role, but is not meaningless. Depending from the size and the possible formation of hydrogen bonds various topological arrangement or distortion variants are realized.

This contribution deals with the synthesis of  $\text{NH}_4[\text{B}(\text{S}_2\text{O}_7)_2]$  as the first ammonium containing borosulfates, which continues previous reported borodisulfates  $A[\text{B}(\text{S}_2\text{O}_7)_2]$  ( $A = \text{Li}, \text{Na}, \text{K}$ ). The investigation of the thermal decomposition products enabled the synthesis of the new compounds  $\text{Na}[\text{B}(\text{SO}_4)_2]$  and  $\text{K}[\text{B}(\text{SO}_4)_2]$  with a chain structure. Additionally, it is shown that the release of  $\text{SO}_3$  is reversible. The formerly known  $\text{Li}[\text{B}(\text{SO}_4)_2]$  was transferred to  $\text{Li}_5[\text{B}(\text{SO}_4)_4]$ . Finally the vibrational spectra of the chain structures  $A[\text{B}(\text{SO}_4)_2]$  ( $A = \text{Na}, \text{K}, \text{NH}_4$ ) are discussed.

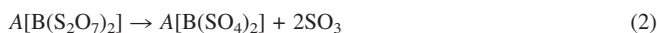
## Results and Discussion

### Synthetic Access to Borosulfates and Relations between Different Compositions

Reactions in oleum favor the formation of condensed sulfate groups and a high B:S ratio according to the high activity of  $\text{SO}_3$  and the hygroscopic properties. By that way borosulfates with disulfate ligands  $A[\text{B}(\text{S}_2\text{O}_7)_2]$  ( $A = \text{Li}, \text{Na}, \text{K}, \text{NH}_4$ ) were obtained according to Equation (1) with oleum as a source for  $\text{SO}_3$  and a sink for  $\text{H}_2\text{O}$ :

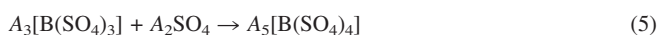
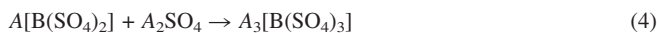


Heating of the disulfate complexes leads to a loss of  $\text{SO}_3$  according to Equation (2):



The loss of  $\text{SO}_3$  can also be achieved by application of a vacuum or may occur in the course of the separation of the reaction products. Generally, the release of  $\text{SO}_3$  should lead to a condensation or a higher degree of connectivity of the  $\text{BO}_4$  tetrahedra. In the case of reaction (2) the change from a ratio 1:4 to a ratio 1:2 should result in a transfer from a structure with isolated pentameric units to a condensed system.

The increase of the B:S ratio is possible by the uptake of  $\text{SO}_3$  and/or  $\text{A}_2\text{SO}_4$  after the following reactions:



For  $A = \text{Li}$  we have recently shown, that  $\text{Li}[\text{B}(\text{SO}_4)_2]$  is obtained by decomposition of  $\text{Li}[\text{B}(\text{S}_2\text{O}_7)_2]$ .<sup>[2]</sup> The crystal structure has a 3D net of tetrahedra with common corners. The arrangement of  $\text{BO}_4$  and  $\text{SO}_4$  tetrahedra is closely related to the  $\text{SiO}_2$  variant  $\beta$ -tridymite. On the other hand a 1D topology was found for  $(\text{H}_3\text{O})[\text{B}(\text{SO}_4)_2]$ . With respect to the  $\text{BS}_4$  super tetrahedra the linear chain with edge-sharing  $\text{SiS}_4$ -tetrahedra in difference to the 3D net of tridymite.

The successful synthesis of  $\text{NH}_4[\text{B}(\text{S}_2\text{O}_7)_2]$  follows reaction (1). The decomposition of the disulfate compounds  $A[\text{B}(\text{S}_2\text{O}_7)_2]$  ( $A = \text{Na}, \text{K}, \text{NH}_4$ ) yields in all cases  $A[\text{B}(\text{SO}_4)_2]$  [reaction (2)]. The back reaction, i.e. the increase of the B:S ratio by the formal uptake of  $\text{SO}_3/\text{A}_2\text{SO}_4$  [reactions (3)–(5)] was observed for the first time in the case of  $\text{Li}_5[\text{B}(\text{SO}_4)_4]$ .

The reactions (1) to (5) assume equilibria between  $\text{A}_2\text{SO}_4/\text{B}(\text{OH})_3/\text{SO}_3$ . It is obvious, that the situation is much more complicated, because other species like  $\text{B}_2\text{O}_3$ ,  $\text{AHSO}_4$ , or  $\text{H}_2\text{SO}_4$  are ignored. It is known from our previous work<sup>[2,3]</sup> they have an impact, too. So the field for variations of the experimental conditions and therefore the access to new borosulfates is wide open.

### Crystal Structure of $\text{NH}_4[\text{B}(\text{S}_2\text{O}_7)_2]$

The first ammonium borosulfate  $\text{NH}_4[\text{B}(\text{S}_2\text{O}_7)_2]$ , crystallizes isotypically with  $\text{K}[\text{B}(\text{S}_2\text{O}_7)_2]$ <sup>[2]</sup> in the space group  $Cc$ . The crystal structure consists of  $[\text{B}(\text{S}_2\text{O}_7)_2]^-$  anions and  $[\text{NH}_4]^+$  cations arranged in an CsCl-like manner.

The remarkable bis(disulfato)borate anion is built up by a central boron atom that is (pseudo)tetrahedrally coordinated by two disulfate units acting as chelate-ligands forming a loop or cyclo (these terms are equal in this case) branched pentamer (Figure 1 and Figure 2). As known from other borosulfates containing disulfate units or from the disulfate complexes reported by Wickleder<sup>[8]</sup> the sulfate tetrahedra comprise three different bond length regimes. The shortest bonds (1.379–1.415 Å) are those between sulfur and the terminal oxygen atoms. The  $\text{S}-\text{O}^{\text{br}}$  bonds to bridging oxygen atoms are shorter for  $\text{S}-\text{O}^{\text{br}}(-\text{B})$  bridges with 1.508–1.538 Å compared with those determined for  $\text{S}-\text{O}^{\text{br}}(-\text{S})$  bridges (1.604–1.629 Å). Like the bond lengths also the  $\text{O}-\text{S}-\text{O}$  angles show three different characteristic ranges, too, increasing from the  $\text{O}^{\text{br}}-\text{S}-\text{O}^{\text{br}}$  ones (99.8–103.0°) via  $\text{O}^{\text{br}}-\text{S}-\text{O}^{\text{term}}$  angles (102.8–113.1°) to  $\text{O}^{\text{term}}-\text{S}-\text{O}^{\text{term}}$  angles (120.4–121.6°). The bond lengths and angles

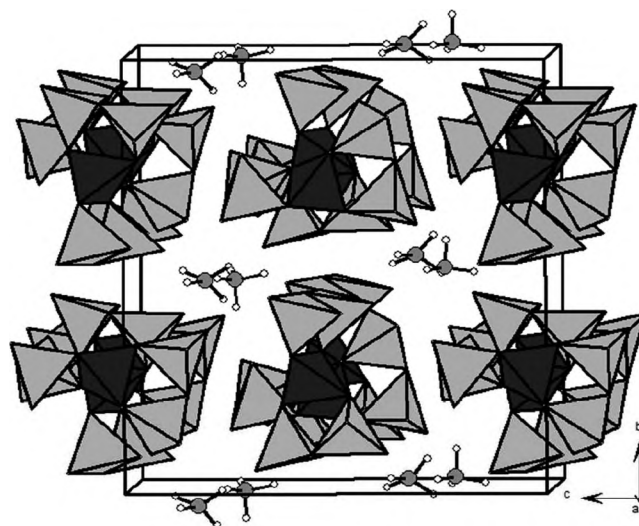


**Figure 1.** Unit cell of  $\text{NH}_4[\text{B}(\text{S}_2\text{O}_7)_2]$ ;  $\text{BO}_4$  (dark grey) and  $\text{SO}_4$  (light grey) tetrahedra form a pentameric unit with two  $(\text{S}_2\text{O}_7)$  groups.

inside the  $\text{BO}_4$  tetrahedra are with 1.379–1.415 Å and 105.5–112.9° in a usual range for borosulfates. The two crystallographically independent pentameric anions exhibit different conformations. In the unit centered by B1 the two six-membered “dreier” rings show a boat conformation with staggered disulfate units (torsions angles 147/148°). In the other, centered by B2, one ring shows chair conformation with an eclipsed disulfate arrangement ( $\tau = 5^\circ$ ) and one boat conformation, with a staggered disulfate unit ( $\tau = 147^\circ$ ).

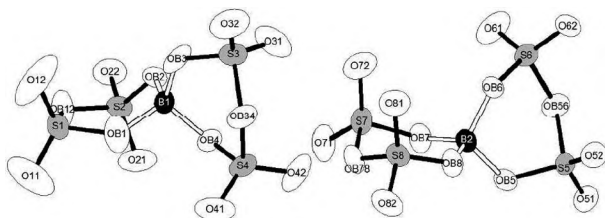


**Figure 2.** Different conformations of the pentameric  $[\text{B}(\text{S}_2\text{O}_7)_2]^-$  anions in  $\text{NH}_4[\text{B}(\text{S}_2\text{O}_7)_2]$ ; ellipsoids are set to 75% probability.

The position of the hydrogen atoms of the ammonium cations were localized by difference Fourier syntheses and were commonly refined with a fixed distance of 100.9 Å to the nitrogen atom. The two crystallographic different ammonium cations are involved in a hydrogen bonding with the terminal oxygen atoms of the pentameric anion as shown in Figure 3. All hydrogen bonds can be classified as medium.<sup>[9]</sup> Minimum  $\text{N}\cdots\text{O}$  distances are 2.85 Å.

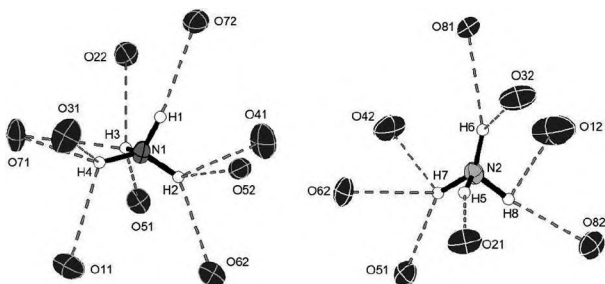


**Figure 3.** Hydrogen bonds in  $\text{NH}_4[\text{B}(\text{S}_2\text{O}_7)_2]$ ; ellipsoids are set to 75% probability.

### Crystal Structure of $\text{Li}_5[\text{B}(\text{SO}_4)_4]$

$\text{Li}_5[\text{B}(\text{SO}_4)_4]$  adopts space group  $P2_1/c$  and crystallizes in a new structure type. The structure comprises open branched pentamers  $[\text{B}(\text{SO}_4)_4]^{5-}$ , where the central boron atom is tetrahedrally surrounded by sulfate groups and  $\text{Li}^+$  cations (Figure 4).

The  $\text{Li}^+$  cations are tetrahedrally coordinated by oxygen forming a layer structure by sharing common edges and corners. The bond lengths inside the sulfate moieties split into two ranges. The bond lengths from sulfur to the terminal oxygen atoms are with 1.426 to 1.483 Å shorter than the bond lengths to the bridging oxygen atoms (1.501–1.574 Å). Like the bond lengths also the  $\text{O}-\text{S}-\text{O}$  angles show two distinct ranges. As known from other condensed sulfates, smaller

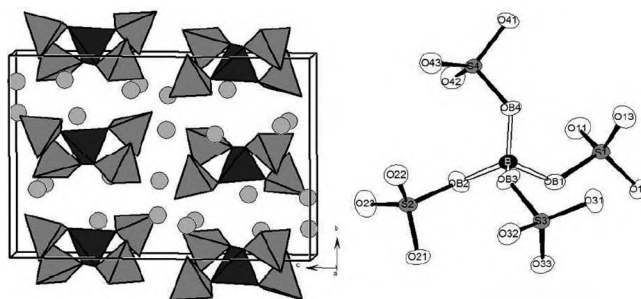


**Figure 4.** Left: Unit cell of  $\text{Li}_5[\text{B}(\text{SO}_4)_4]$ ;  $\text{BO}_4$  and  $\text{SO}_4$  tetrahedra are drawn as dark and light gray polyhedra. Right: Open branched pentameric  $[\text{B}(\text{SO}_4)_4]^{5-}$  anion; ellipsoids are set to 75% probability.

angles are found for the angles  $\text{O}^{\text{br}}-\text{S}-\text{O}^{\text{term}}$  (105.6–109.8) and for  $\text{O}^{\text{term}}-\text{S}-\text{O}^{\text{term}}$  (108.2–115.8°) ones. The bond lengths and angles in the  $\text{BO}_4$  tetrahedra lie with 1.443–1.494 Å and 105.7–113.9° also in a normal range for borosulfates. The conformation of the pentameric anion can be described by the torsion angles of the terminal sulfate tetrahedra to the central  $\text{BO}_4$  unit. Therefore, all  $\text{SO}_4$  groups are arranged in a staggered manner with respect to the  $\text{BO}_4$  unit ( $\tau = 160\text{--}172^\circ$ ); this conformation is the same as found in  $\text{Na}_5[\text{B}(\text{SO}_4)_4]\cdot\text{I}$ .<sup>[2]</sup>

As mentioned above, all  $\text{Li}^+$  cations are tetrahedrally coordinated by terminal oxygen atoms, but the two  $\text{Li}^+$  cations Li1 and Li3 might be better described with a 4+1 coordination forming capped tetrahedra with the fifth oxygen atom being 2.44–2.48 Å apart, compared with the other four (1.90 to 2.19 Å).  $(\text{Li}2)\text{O}_4$  and  $(\text{Li}3)\text{O}_5$  share a common edge.  $(\text{Li}1)\text{O}_5$  links this unit by common corners forming a “dreier” ring.  $(\text{Li}4)\text{O}_4$  and  $(\text{Li}5)\text{O}_4$  connect the “dreier” rings by sharing corners to layers. Despite its lower coordination numbers, the tetrahedrally coordinated  $\text{Li}^+$  cations have a higher bond valence sum<sup>[10]</sup> (1.08–1.13) than Li1 (0.96) and Li3 (0.98) (Figure 5).

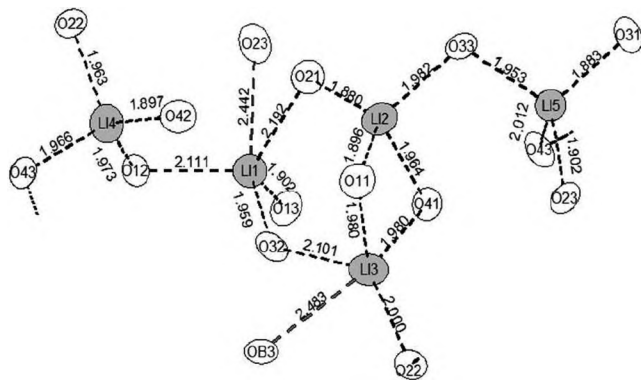


**Figure 5.** Coordination of the  $\text{Li}^+$  cations in  $\text{Li}_5[\text{B}(\text{SO}_4)_4]$ , ellipsoids are set to 75% probability.

### Crystal Structures of $A[\text{B}(\text{SO}_4)_2]$ ( $A = \text{Na}, \text{K}, \text{NH}_4$ )

Compounds  $A[\text{B}(\text{SO}_4)_2]$  ( $A = \text{K}, \text{NH}_4$ ) crystallize isotypically with  $\text{H}_3\text{O}[\text{B}(\text{SO}_4)_2]$  in the space group  $P4/mcc$ .  $\text{Na}[\text{B}(\text{SO}_4)_2]$  (space group  $P2_1/c$ ) forms a new structure type. Both crystal structures consist of a rod packing of the loop

branched “vierer” single chain with the cations in the resulting channels. As Figure 6 shows the main difference results from twist angle within the chain.

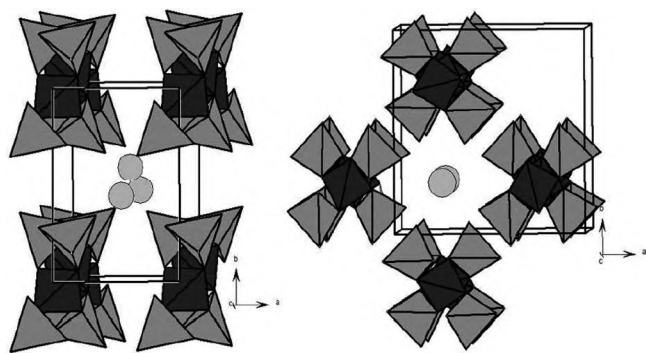


**Figure 6.** Left: Unit cell of Na[B(SO<sub>4</sub>)<sub>2</sub>] right: Unit cell of K[B(SO<sub>4</sub>)<sub>2</sub>]. BO<sub>4</sub> and SO<sub>4</sub> tetrahedra are shown as dark and light gray polyhedra, respectively.

In A[B(SO<sub>4</sub>)<sub>2</sub>] (A = K, NH<sub>4</sub>), the SO<sub>4</sub> tetrahedra of the chain are rotated by 90° according to the space group symmetry. The orientation to the neighbored chains is in a way that the tetrahedra are always on different heights. The BS<sub>4</sub> super tetrahedra are nearly regular (Table 1).

In Na[B(SO<sub>4</sub>)<sub>2</sub>] the chain shows a clear deviation from  $\bar{4}$  symmetry. This results from a strong twist of the [B(SO<sub>4</sub>)<sub>4</sub>] units, so the angle amounts to about 45° instead of an idealized value of 90°. This is also visible in the strong deviation of 45% for the BS<sub>4</sub> super tetrahedron (Table 1). According to the small size of the unit cell every borosulfate chain is congruent to the neighbored ones. The twist of the chain in Na[B(SO<sub>4</sub>)<sub>2</sub>] can be seen as the start of the interaction between the chains as a result of the small size of Na<sup>+</sup>. This might explain, why Li[B(SO<sub>4</sub>)<sub>2</sub>], which is obtained in a similar way by thermal decomposition of Li[B(S<sub>2</sub>O<sub>7</sub>)<sub>2</sub>] adopts not a chain structure but a 3D net of tetrahedra.<sup>[2]</sup>

Again, as expected from the topology, the bond lengths in the sulfate tetrahedra are split into two ranges. The bonds from

sulfur to the terminal oxygen atoms with approx. 1.42 Å are shorter than the bonds to the bridging oxygen atoms with 1.52 Å (Na) to 1.54 Å (K, NH<sub>4</sub>). The bond angles O–S–O show three different ranges. Smallest angles are found from O<sup>br</sup>–S–O<sup>br</sup> 103° (Na) to 105° (NH<sub>4</sub>), slightly larger for O<sup>br</sup>–S–O<sup>term</sup> with ca. 105–111° and the largest for O<sup>term</sup>–S–O<sup>term</sup> with 118°. Bond lengths and angles in the BO<sub>4</sub> tetrahedra range between 1.30 Å (Na) to 1.28 Å (K, NH<sub>4</sub>) and from 102 to 116°, normal ranges for borosulfates. BO<sub>4</sub> and SO<sub>4</sub> tetrahedra are nearly regular with the greatest deviations for the BO<sub>4</sub> tetrahedron in Na[B(SO<sub>4</sub>)<sub>2</sub>].

The different twist angles affect also the arrangement within the chain. The conformations of the eight membered “vierer” ring in A[B(SO<sub>4</sub>)<sub>2</sub>] (A = K, NH<sub>4</sub>) adopt a boat conformation with the sulfates tetrahedra arranged eclipsic with respect to the borate tetrahedra ( $\tau = 4^\circ$ ), whereas in Na[B(SO<sub>4</sub>)<sub>2</sub>] a boat-chair conformation with staggered BO<sub>4</sub> and SO<sub>4</sub> units is found ( $\tau = 179^\circ$ ) (Figure 7, Figure 8).

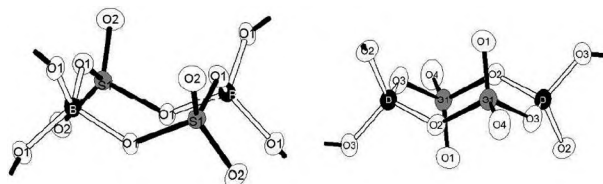


**Figure 7.** Different conformations of the polymeric anions in A[B(SO<sub>4</sub>)<sub>2</sub>] (A = K, NH<sub>4</sub>) (left) and Na[B(SO<sub>4</sub>)<sub>2</sub>] (right); ellipsoids are set to 75% probability.

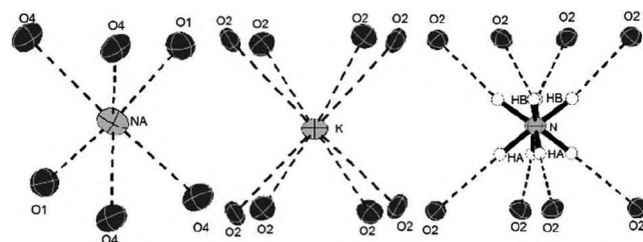


**Figure 8.** Coordination of the A<sup>+</sup> cations in A[B(SO<sub>4</sub>)<sub>2</sub>]; ellipsoids are set to 75% probability.

**Table 1.** Calculated deviations /% from ideal symmetry for borosulfates according to reference<sup>[7]</sup>.

Compound	BO <sub>4</sub>	SO <sub>4</sub>	S <sub>2</sub> O <sub>7</sub>	BS <sub>4</sub>	Reference
Li <sub>5</sub> [B(SO <sub>4</sub> ) <sub>4</sub> ]	0.45	0.24–0.62		25.0	this work
Na <sub>5</sub> [B(SO <sub>4</sub> ) <sub>4</sub> ]-I	1.22 / 1.32	0.07–0.20		14.6	[2]
Na <sub>5</sub> [B(SO <sub>4</sub> ) <sub>4</sub> ]-II	0.46	0.10–0.35		44.3 / 45.4	[2]
K <sub>5</sub> [B(SO <sub>4</sub> ) <sub>4</sub> ]	0.43	0.08–0.23		4.1	[2]
H[B(SO <sub>4</sub> )(S <sub>2</sub> O <sub>7</sub> )]	0.15/0.32	0.40/0.53	0.11–0.20	24.5 / 25.6	[3]
Cs[B(SO <sub>4</sub> )(S <sub>2</sub> O <sub>7</sub> )]	0.38	0.31	0.14 / 0.17	26.2	[3]
K <sub>3</sub> [B(SO <sub>4</sub> ) <sub>3</sub> ]	0.58	0.11 / 0.55		3.1	[2]
Rb <sub>3</sub> [B(SO <sub>4</sub> ) <sub>3</sub> ]	0.65	0.14 / 0.76		2.8	[2]
Li[B(S <sub>2</sub> O <sub>7</sub> ) <sub>2</sub> ]	0.26 / 0.98		0.07–0.28	39.0 / 58.7	[2]
Na[B(S <sub>2</sub> O <sub>7</sub> ) <sub>2</sub> ]	0.33		0.07–0.16	45.0	[3]
K[B(S <sub>2</sub> O <sub>7</sub> ) <sub>2</sub> ]	0.10 / 0.34		0.08–0.22	36.9 / 45.3	[3]
NH <sub>4</sub> [B(S <sub>2</sub> O <sub>7</sub> ) <sub>2</sub> ]	0.15 / 0.35		0.07–0.21	37.5 / 44.4	this work
H <sub>3</sub> O[B(SO <sub>4</sub> ) <sub>2</sub> ]	0.31	0.26		5.0	[3]
Na[B(SO <sub>4</sub> ) <sub>2</sub> ]	1.27	0.19		40.5	this work
K[B(SO <sub>4</sub> ) <sub>2</sub> ]	0.32	0.23		4.4	this work
NH <sub>4</sub> [B(SO <sub>4</sub> ) <sub>2</sub> ]	0.20	0.28		5.5	this work
Li[B(SO <sub>4</sub> ) <sub>2</sub> ]	0.19 / 0.33	0.13–0.55		1.5 / 2.4	[2]
B <sub>2</sub> S <sub>2</sub> O <sub>9</sub>	0.32	0.34		0.67	[5]

In  $K[B(SO_4)_2]$  the potassium atoms are eight fold coordinated by terminal oxygen atoms with the distances of 2.777 ( $4 \times$ ) and 2.887 ( $4 \times$ ) Å. The polyhedron is a nearly regular cube. In  $NH_4[B(SO_4)_2]$  the positions of the hydrogen atoms of the ammonium cations were localized by difference Fourier syntheses and fixed with a distance of 1.009 Å to the nitrogen atom. Similar to the isotopic oxonium compound  $H_3O[B(SO_4)_2]$  the hydrogen atoms are disordered. According to symmetry and multiplicity the four hydrogen atoms are distributed on eight positions around the nitrogen atom with a refined occupation factor of 0.5. The N–O distance is consistent with a moderate hydrogen bond. In  $Na[B(SO_4)_2]$  the sodium atoms are six fold coordinated as a trigonal prism by terminal oxygen atoms in the range of 2.32–2.54 Å.

The isotypism between potassium, ammonium, and oxonium compound, which is very rare in solid state chemistry, enables an estimation of the volume and ionic radius of the oxonium cation. According to lattice parameter and unit cell volume the size of  $H_3O^+$  in between  $NH_4^+$  and  $K^+$ , but slightly closer to  $NH_4^+$ .

### Deviations from Ideal Symmetry

Deviations from ideal symmetry were calculated applying the method of all ligands enclosing spheres. In a first step the optimum centroid of the four surrounding oxygen atoms is determined by a least-square refinement and gives a medium centroid–ligand distance. Subsequently, the volume of an ideal tetrahedron is calculated using this distance. Finally, this volume is compared to the experimentally obtained tetrahedron.<sup>[7]</sup> Table 1 shows the deviations for all herein reported borosulfate anions and  $B_2S_2O_9$ . Usually the deviations of  $BO_4$  and  $SO_4$  tetrahedra are below or near 0.5% and can be classified as regular.

The deviations for the super-tetrahedra are strongly influenced by the respective conformation of the anions. While the  $BS_4$  units in  $A[B(SO_4)_2]$  ( $A = K, NH_4, H_3O$ ) are quite regular,  $Na[B(SO_4)_2]$  shows a large distortion (5% vs. 40%). Also the orientation of the tetrahedra in  $Li_5[B(SO_4)_4]$  that is the same orientation as in  $Na_5[B(SO_4)_4]$ -I seem to cause high deviations, while the deviation for  $K_5[B(SO_4)_4]$  that adopts another conformation amount only ca. 5%. For  $A[B(S_2O_7)_2]$  ( $A = Li - K$ ) all known compounds (with also different conformations) have great deviations, that is clearly caused by the  $S_2O_7$  units. The same is true for the chain structures of  $A[B(SO_4)(S_2O_7)]$  ( $A = H, Cs$ ), but according to the different share of  $S_2O_7$  units, the deviation is reduced. Crystal structures, which come directly from silicate structures  $\{Li[B(SO_4)_2], B_2S_2O_9\}$  show remarkably small deviations. A minor influence comes from the size of the cations. For compounds with  $A = K, NH_4$  and  $H_3O$  the deviations are quite small (for the absence of disulfates), while all species with sodium are distorted.

### Vibrational Spectroscopy of $A[B(SO_4)_2]$ ( $A = Na, K, NH_4$ )

Figure 9 shows infrared and Raman spectra of  $A[B(SO_4)_2]$  ( $A = Na, K, NH_4$ ). Because of the same topology the observed

spectra are very similar. In the infrared spectra, the strong bands at around  $1350\text{ cm}^{-1}$  come from overlap of  $\nu_{as}(SO_2, \text{terminal})$  and  $\nu(BO_4)$ . The medium bands around  $1200\text{ cm}^{-1}$  can be assigned to the  $\nu_s(SO_2, \text{terminal})$  vibrations. The very broad bands in the region of  $1060$  to  $850\text{ cm}^{-1}$  are mainly influenced by the bridging vibrations  $\nu_{as}(S-O-B)$ . The bands below that region are from the wagging vibration of the  $SO_4$  group. Strong N–H modes of  $NH_4[B(SO_4)_2]$  are around  $3300\text{ cm}^{-1}$ . The Raman spectra of all compounds are well resolved. Modes of medium intensity around  $1340\text{ cm}^{-1}$  are assigned to  $\nu_{as}(SO_2, \text{terminal})$ . The strong bands at  $1238\text{ cm}^{-1}$  ( $1255\text{ cm}^{-1}$ , Na) come from the symmetric bending vibrations of the terminal oxygen to sulfur  $\nu_{as}(SO_2)$ . The very strong band at  $1060\text{ cm}^{-1}$  ( $1080\text{ cm}^{-1}$ , Na) are a mixture from  $\nu(SO_4)$  and  $\nu(BO_4)$ . The bands in the range from  $715$  to  $380\text{ cm}^{-1}$  are mainly influenced by wagging modes from the sulfate groups and the bands from  $330$  to  $150\text{ cm}^{-1}$  from the borate group. The greatest difference for the two different structure types is reflected in the Raman spectra for the very strong band at  $613\text{ cm}^{-1}$  ( $NH_4, K$ ) and  $711\text{ cm}^{-1}$  (Na). This striking shift results from the different conformation of the chains, because the force constants are comparable. Furthermore, due to the calculations both modes are strongly correlated to the S–O–B deformation.

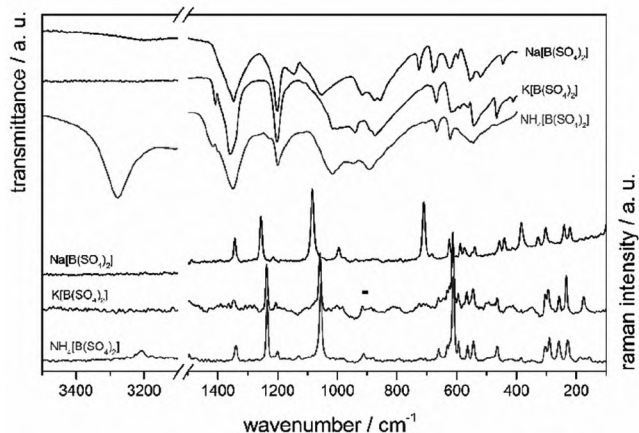


**Figure 9.** Infrared (top) and Raman spectra (bottom) of  $A[B(SO_4)_2]$  ( $A = Na, K, NH_4$ ).

Table 2 shows the calculated force constants with the program VIBRATZ.<sup>[11]</sup> Because of the formal increase of the bond order for the terminal oxygen atoms, the bond forces for the  $S-O^{\text{term}}$  bonds in  $A[B(SO_4)_2]$  ( $A = Na, K, NH_4$ ) are significantly higher than in  $K_5[B(SO_4)_4]$  and therefore comparable with other force constants containing  $(SO_2^{\text{term}})$  units.<sup>[12]</sup> The force constants of the terminal S–O bonds show a general tendency according to the connectivity and therefore the B:S ratio. Lowest values are observed for the compounds with isolated pentamers, medium for  $K_3[B(SO_4)_3]$  and higher values for the chain structures  $A[B(SO_4)_2]$ . The maximum represents the disulfate compound  $Li[B(S_2O_7)_2]$ .

### Conclusions

Starting two years ago with  $K_5[B(SO_4)_4]$  as the first representative borosulfates have emerged as a well-established class

**Table 2.** Calculated force constants /mdyn·Å<sup>-1</sup> for borosulfates.

Compound	$f(\text{S-O}^{\text{term}})$	$f(\text{S-O}^{\text{br}})$	$f(\text{B-O})$	$d(\text{SO})$	$d(\text{BO})$
Na[B(SO <sub>4</sub> ) <sub>2</sub> ]	9.1	4.7	3.5	0.8	0.5
K[B(SO <sub>4</sub> ) <sub>2</sub> ]	9.4	4.7	3.5	0.8	0.5
NH <sub>4</sub> [B(SO <sub>4</sub> ) <sub>2</sub> ]	9.4	4.7	3.5	0.8	0.5
K <sub>3</sub> [B(SO <sub>4</sub> ) <sub>3</sub> ]	8.7	4.9	3.2	0.6	0.5
K <sub>5</sub> [B(SO <sub>4</sub> ) <sub>4</sub> ]	7.9	4.7	3.3	0.7	0.5
Na <sub>5</sub> [B(SO <sub>4</sub> ) <sub>4</sub> ]	8.0	4.8	3.3	0.7	0.5
Li[B(S <sub>2</sub> O <sub>7</sub> ) <sub>2</sub> ]	9.8	4.8/3.7	3.6	0.7	0.5

of compounds. Because the crystal structures only contain BO<sub>4</sub> and SO<sub>4</sub> tetrahedra connected via common apices, there are close relations to silicates, but some new features, too.

This contribution shows that borosulfates have a remarkable flexibility with respect to composition, topology, and coordination arrangement. At first, borosulfates are characterized for nearly all univalent cations *A* with *A* = Li, Na, K, Rb, Cs, NH<sub>4</sub>, H<sub>3</sub>O, H. Herein we record the first time on ammonium compounds. According to the different coordinations of *A* there are examples for isotypism, distortion variants, and topological variants. At second, the diversity is achieved although all borosulfates have one common feature: There are only tetrahedral BO<sub>4</sub> and SO<sub>4</sub> units and the BO<sub>4</sub> tetrahedron is always tetrahedrally surrounded by SO<sub>4</sub> units forming a “BS<sub>4</sub> super tetrahedron” (BBS<sub>3</sub> in B<sub>2</sub>S<sub>2</sub>O<sub>9</sub>).

The most important issue is the ratio between BO<sub>4</sub> and SO<sub>4</sub> tetrahedra. With a ratio 1:2 the compounds A[B(SO<sub>4</sub>)<sub>2</sub>] form a 1D structure for *A* = Na, K, NH<sub>4</sub>. Probably as a matter of the cation's size K[B(SO<sub>4</sub>)<sub>2</sub>] and NH<sub>4</sub>[B(SO<sub>4</sub>)<sub>2</sub>] are isotypic and the chains have an undistorted  $\bar{4}$  symmetry like the oxonium compound. Against this, the chain in Na[B(SO<sub>4</sub>)<sub>2</sub>] shows a distinctive twist, i.e. the angle between SO<sub>4</sub> tetrahedra is 45° instead of 90°. The analogous Li compound forms not a chain structure but a 3D network related to the SiO<sub>2</sub> polymorph β-tridymite.

Isolated pentameric units [B(SO<sub>4</sub>)<sub>4</sub>]<sup>5-</sup> are now known for *A* = Li, Na, K. Differences between the particular structures result from the coordination of the cation. The distortion of the BS<sub>4</sub> super tetrahedra increases with decreasing size of *A*. The (probably) metastable Na<sub>5</sub>[B(SO<sub>4</sub>)<sub>4</sub>]-II is not yet fully understood.<sup>[2]</sup>

A B:S ratio of 1:4 is also found in disulfate compounds A[B(S<sub>2</sub>O<sub>7</sub>)<sub>2</sub>]. The condensation of the SO<sub>4</sub> tetrahedra reduces the charge of the complex anion and distorts the BS<sub>4</sub> tetrahedra. Again, ammonium and potassium compound are isotypic, while own structure types are found for *A* = Li or Na. In each case the thermal decomposition of A[B(S<sub>2</sub>O<sub>7</sub>)<sub>2</sub>] results in compounds A[B(SO<sub>4</sub>)<sub>2</sub>].

The relations between borosulfates of different B:S ratio is not limited to aspects of the structural chemistry, but extends also to the synthetic approach. Besides the thermal decomposition and a condensation/hydrolysis to/of disulfate groups in combination with protonation/deprotonation there is also the possibility for the “uptake” of SO<sub>3</sub>/A<sub>2</sub>SO<sub>4</sub> as shown for the first time for Li<sub>5</sub>[B(SO<sub>4</sub>)<sub>4</sub>].

Additionally, we presented vibrational spectra and determined force constants by fitting calculated spectra to the experimental data. As expected there is a correlation between the degree of condensation of the SO<sub>4</sub> tetrahedra and the force constant of the terminal S–O bonds. This is of interest for a better understanding for the structures of borosulfate glasses.<sup>[13]</sup>

Finally, framework structures of oxo compounds are the most important materials for applications with respect to optical properties. In this field borosulfates may perform new features.<sup>[11]</sup> First patents for borosulfates as new optical materials were already claimed.<sup>[14]</sup>

## Experimental Section

**Syntheses:** NH<sub>4</sub>[B(S<sub>2</sub>O<sub>7</sub>)<sub>2</sub>] was prepared by adding ammonium sulfate (NH<sub>4</sub>)<sub>2</sub>SO<sub>4</sub> (0.70 g, 5.3 mmol, Merck, p.a.) and boron acid B(OH)<sub>3</sub> (0.64 g, 10.3 mmol, ABCR, 99.6 %) to oleum (10 mL, Merck, 65 % SO<sub>3</sub>). After one week the precipitate was collected.

A[B(SO<sub>4</sub>)<sub>2</sub>] (*A* = Na, K, NH<sub>4</sub>) were prepared starting from the corresponding borosulfate complex A[B(S<sub>2</sub>O<sub>7</sub>)<sub>2</sub>] in oleum. By removing these complexes from oleum under an oil pump vacuum a decomposition reaction analog Equation (2) is starting. For a better crystallization and to remove residuals of sulfuric acid the samples were heated in silica crucibles on air up to 573 K overnight.

Li<sub>5</sub>[B(SO<sub>4</sub>)<sub>4</sub>] was prepared starting from Li[B(S<sub>2</sub>O<sub>7</sub>)<sub>2</sub>] in oleum and sucked of using a membrane pump. The very “wet” (i.e. oleum containing) precipitate was placed in a silica crucibles and heated on air up to 573 K overnight.

**Crystal Structure Analyses:** Suitable single crystals of all title compounds were selected under a polarizing microscope and enclosed in glass capillaries under perflourated oil. X-ray diffraction data were collected with a Bruker Quazar/APEX II with a CCD detector.<sup>[15]</sup> The data were corrected for absorption by multi-scan.<sup>[16]</sup> The crystal structures were solved by direct methods and refined using SHELXTL.<sup>[17]</sup> In all cases refinements were performed with anisotropic displacement parameters for all non hydrogen atoms. Crystallographic data and further details of the X-ray data collection are summarized in Table 3. Selected distances and angles are given in Table 4. Coordinates and displacement parameters are listed in the Supporting Information.

Further details of the crystal structures investigations may be obtained from the Fachinformationszentrum Karlsruhe, 76344 Eggenstein-Leopoldshafen, Germany (Fax: +49-7247-808-666; E-Mail: crysdata@fiz-karlsruhe.de, <http://www.fiz-karlsruhe.de/request> for deposited data.html) on quoting the depository numbers CSD-428001

**Table 3.** Crystallographic data (estimated standard deviations in parentheses).

	Li <sub>5</sub> [B(SO <sub>4</sub> ) <sub>4</sub> ]	NH <sub>4</sub> [B(S <sub>2</sub> O <sub>7</sub> ) <sub>2</sub> ]	NH <sub>4</sub> [B(SO <sub>4</sub> ) <sub>2</sub> ]	K[B(SO <sub>4</sub> ) <sub>2</sub> ]	Na[B(SO <sub>4</sub> ) <sub>2</sub> ]
Temperature /K	293(2)	150(2)	150(2)	293(2)	293(2)
Crystal system	monoclinic	monoclinic	tetragonal	tetragonal	monoclinic
Space group	<i>P</i> 2 <sub>1</sub> / <i>c</i>	<i>Cc</i>	<i>P</i> 4/ <i>ncc</i>	<i>P</i> 4/ <i>ncc</i>	<i>P</i> 2/ <i>c</i>
<i>a</i> /Å	8.0191(1)	11.4403(2)	9.1980(1)	8.9739(3)	5.434(5)
<i>b</i> /Å	10.1211(1)	14.9439(2)			7.570(7)
<i>c</i> /Å	15.0401(2)	13.8693(2)	7.4258(1)	7.4114(3)	7.766(8)
$\beta$ /°	104.033(1)	93.662(1)			99.74(2)
<i>V</i> /Å <sup>3</sup>	1184.25(3)	2366.29(6)	628.22(2)	596.85(5)	207.52(7)
<i>Z</i>	4	8	4	4	2
Calc. density <i>D</i> <sub>x</sub> /g·cm <sup>-3</sup>	2.410	2.139	2.336	2.693	2.477
$\mu$ Mo- <i>K</i> <sub>α</sub> /mm <sup>-1</sup>	0.900	0.883	0.861	1.595	0.955
Radiation			Mo- <i>K</i> <sub>α</sub> radiation		
Diffractometer			Bruker APEX-2		
Absorption correction			multi-scan		
Index range	-12 ≤ <i>h</i> ≤ 12, -14 ≤ <i>k</i> ≤ 15, -23 ≤ <i>l</i> ≤ 23	-16 ≤ <i>h</i> ≤ 16, -20 ≤ <i>k</i> ≤ 20, -19 ≤ <i>l</i> ≤ 18	-11 ≤ <i>h</i> ≤ 12, -12 ≤ <i>k</i> ≤ 12, -10 ≤ <i>l</i> ≤ 10	-15 ≤ <i>h</i> ≤ 16, -16 ≤ <i>k</i> ≤ 12, -13 ≤ <i>l</i> ≤ 13	-7 ≤ <i>h</i> ≤ 8, -10 ≤ <i>k</i> ≤ 11, -6 ≤ <i>l</i> ≤ 11
Theta range ( $\theta_{\min}$ – $\theta_{\max}$ )	2.45–33.44	2.25–30.00	3.13–29.93	3.21–39.90	2.69–33.72
Reflections collected	4308	16991	8402	10286	10701
Independent reflections	3778	5263	463	909	605
Parameters	236	386	36	30	56
<i>R</i> <sub>int</sub> / <i>R</i> <sub>sigma</sub>	0.020 / 0.018	0.036 / 0.039	0.032 / 0.013	0.041 / 0.022	0.018 / 0.028
<i>R</i> -values	<i>R</i> <sub>1</sub> = 0.025 <i>wR</i> <sub>2</sub> = 0.074	<i>R</i> <sub>1</sub> = 0.033 <i>wR</i> <sub>2</sub> = 0.068	<i>R</i> <sub>1</sub> = 0.022 <i>wR</i> <sub>2</sub> = 0.069	<i>R</i> <sub>1</sub> = 0.023 <i>wR</i> <sub>2</sub> = 0.060	<i>R</i> <sub>1</sub> = 0.032 <i>wR</i> <sub>2</sub> = 0.091
<i>R</i> <sub>1</sub> (all data)	<i>R</i> <sub>1</sub> = 0.031	<i>R</i> <sub>1</sub> = 0.041	<i>R</i> <sub>1</sub> = 0.024	<i>R</i> <sub>1</sub> = 0.034	<i>R</i> <sub>1</sub> = 0.036
Goodness of fit (GooF)	1.092	1.042	1.168	1.069	1.167
Residual electron density, min/max	-0.447 / 0.558	-0.429 / 0.771	-0.399 / 0.369	-0.436 / 0.671	-0.745 / 0.665
Comments		Inversion twin: BASF = 0.48033			

**Table 4.** Selected distances /Å and angles /° for Li<sub>5</sub>[B(SO<sub>4</sub>)<sub>4</sub>], A[B(SO<sub>4</sub>)<sub>2</sub>] (*A* = Na, K, NH<sub>4</sub>), and NH<sub>4</sub>[B(S<sub>2</sub>O<sub>7</sub>)<sub>2</sub>] (estimated standard deviations in parentheses).

Distances /Å; angles /°	Li <sub>5</sub> [B(SO <sub>4</sub> ) <sub>4</sub> ]	Na[B(SO <sub>4</sub> ) <sub>2</sub> ]	K[B(SO <sub>4</sub> ) <sub>2</sub> ]	NH <sub>4</sub> [B(SO <sub>4</sub> ) <sub>2</sub> ]	NH <sub>4</sub> [B(S <sub>2</sub> O <sub>7</sub> ) <sub>2</sub> ]
A–O	1.880(3)–2.192(3)	2.317(3)–2.541(3)	2.777(1), 2.887(1)	2.878(3), 2.942(3)	2.839(7)–3.163(8)
S–O <sup>term</sup>	1.426(1)–1.483(1)	1.422(3), 1.425(2)	1.4237(7)	1.4228(14)	1.379(4)–1.415(4)
S–O <sup>br</sup> (–S)					1.604(4)–1.629(4)
S–O <sup>br</sup> (–B)	1.501(1)–1.574(1)	1.522(3), 1.530(2)	1.5372(7)	1.5401(13)	1.508(4)–1.538(4)
B–O	1.443(2)–1.494(2)	1.465(3), 1.469(3)	1.4678(7)	1.4690(12)	1.446(7)–1.479(6)
O <sup>term</sup> –S–O <sup>term</sup>	108.17(7)–115.83(6)	117.91(16)	117.74(7)	117.45(12)	120.4(3)–121.6(2)
O <sup>br</sup> –S–O <sup>term</sup>	100.58(5)–109.77(6)	105.84(14)–111.33(14)	105.40(4), 111.35(4)	105.68(7), 111.19(7)	102.8(3)–113.1(2)
O <sup>br</sup> –S–O <sup>br</sup>		103.19(14)	104.95(6)	105.04(10)	99.8(2)–103.0(2)
S–O <sup>br</sup> –S					119.7(2)–123.1(2)
S–O <sup>br</sup> –B	127.94(8)–132.89(8)	130.10(19)	128.78(5)	128.55(9)	119.4(3)–127.3(3)
O–B–O	105.7(1)–113.9(1)	102.33(14)–115.5(3)	107.92(3), 112.63(5)	108.00(5), 112.46(9)	105.5(4)–112.9(4)

(NH<sub>4</sub>[B(S<sub>2</sub>O<sub>7</sub>)<sub>2</sub>]), CSD-428002 (Li<sub>5</sub>[B(SO<sub>4</sub>)<sub>4</sub>]), CSD-428003 (K[B(SO<sub>4</sub>)<sub>2</sub>]), CSD-428004 (NH<sub>4</sub>[B(SO<sub>4</sub>)<sub>2</sub>]), and CSD-428005 (Na[B(SO<sub>4</sub>)<sub>2</sub>]).

**Powder-XRD:** All products were characterized by Powder-XRD (STOE Stadi P, Cu-*K*<sub>α1</sub> radiation, Ge monochromator, image plate detector, Debye-Scherrer setup, transmission). Experimental and calculated diagrams are given in the Supporting Information.

Single phase samples were obtained for A[B(SO<sub>4</sub>)<sub>2</sub>] (*A* = Na, K, NH<sub>4</sub>). The sample of K[B(SO<sub>4</sub>)<sub>2</sub>] was mixed with additional glass powder to obtain reasonable data (needles with texture effects).

Li<sub>5</sub>[B(SO<sub>4</sub>)<sub>4</sub>] occurs only as a minority phase besides an unknown majority phase. This fits to the conditions of the synthesis.

NH<sub>4</sub>[B(S<sub>2</sub>O<sub>7</sub>)<sub>2</sub>] was not isolated because of the decomposition to NH<sub>4</sub>[B(SO<sub>4</sub>)<sub>2</sub>].

**Vibrational Spectroscopy:** Raman spectra were recorded with a Bruker FRA 106/S module with a Nd:YAG laser ( $\lambda$  = 1064 nm). IR spectra were recorded with a Nicolet Magna 760 spectrometer using a Diamond Orbit ATR unit (extended ATR correction with a refraction index of 1.5 was used).

**Supporting Information** (see footnote on the first page of this article): coordinates with standard deviations as refined from single crystal data, observed and calculated XRD powder diffraction patterns and D–A distances for H-bridges in NH<sub>4</sub>-compounds.

## Acknowledgements

The authors thank *Mr. Artur Schick* for recording the Raman spectra

## References

- [1] H. A. Höpfe, K. Kazmierczak, M. Daub, K. Förg, F. Fuchs, H. Hillebrecht, *Angew. Chem.* **2012**, *124*, 6359–6362; *Angew. Chem. Int. Ed.* **2012**, *51*, 6255–6257.
- [2] M. Daub, K. Kazmierczak, P. Gross, H. Höpfe, H. Hillebrecht, *Inorg. Chem.* **2013**, *52*, 6011–6020.
- [3] M. Daub, K. Kazmierczak, H. A. Höpfe, H. Hillebrecht, *Chem. Eur. J.* **2013**, *19*, 16954–16962.
- [4] B. Ewald, Y.-X. Huang, R. Kniep, *Z. Anorg. Allg. Chem.* **2007**, *633*, 1517–1540.
- [5] C. Logemann, M. S. Wickleder, *Angew. Chem.* **2013**, *125*, 14479–14482; *Angew. Chem. Int. Ed.* **2013**, *52*, 14229–14232.
- [6] F. Liebau, *Structural Chemistry of Silicates*, Springer Verlag, Heidelberg, **1985**.
- [7] a) T. Balić-Žunić, E. Makovicky, *Acta Crystallogr., Sect. B* **1996**, *52*, 78–81; b) E. Makovicky, T. Balić-Žunić, *Acta Crystallogr., Sect. B* **1998**, *54*, 766–773.
- [8] a) C. Logemann, D. Gunzelmann, T. Klüner, J. Senker, M. S. Wickleder, *Chem. Eur. J.* **2012**, *18*, 15495–15503; b) C. Logemann, M. S. Wickleder, *Inorg. Chem.* **2011**, *50*, 11111–11116; c) C. Logemann, J. Witt, D. Gunzelmann, J. Senker, M. S. Wickleder, *Z. Anorg. Allg. Chem.* **2012**, *638*, 2053–2061.
- [9] T. Steiner, *Angew. Chem.* **2002**, *114*, 50–80; *Angew. Chem. Int. Ed.* **2002**, *41*, 48–76.
- [10] I. D. Brown, *J. Appl. Crystallogr.* **1996**, *29*, 479–480.
- [11] a) E. Dowty, *Phys. Chem. Miner.* **1987**, *14*, 67–79; b) VIBRATZ 2.2, Shape Software, Kingsport, TN, USA.
- [12] A. Simon, A. Pischtschan, *Z. Anorg. Allg. Chem.* **1966**, *344*, 1–9.
- [13] a) P. Mustarelli, *Solid State Ionics* **1990**, *39*, 217–224; b) P. R. Gandhi, V. K. Deshpande, K. Singh, *Bull. Mater. Sci.* **1992**, *15*, 467–471; c) I. Pal, A. Agarwal, S. Sanghi, A. Sheoran, N. Ahlawat, *J. Alloys Compd.* **2009**, *472*, 40–45.
- [14] Patent application: CN 201310151075, 26.6.2013; patent declaration: CN 103205812 A, 17.7.2013).
- [15] SAINT, Data Reduction and Frame Integration Program for the CCD Area-Detector System, Bruker Analytical X-ray Systems, Madison, WI, USA, **2006**.
- [16] G. M. Sheldrick, *SADABS, Program for Area Detector Adsorption Correction*, Institute for Inorganic Chemistry, University of Göttingen, Germany **1996**.
- [17] G. M. Sheldrick, *SHELXTL*, Bruker AXS Analytical X-ray Instruments Inc, Madison, WI, USA, **1997**.